Published online 5 October 2012 *Nucleic Acids Research, 2012, Vol. 40, No. 22* ***11571–11582***
doi:10.1093/nar/gks898

Pol β associated complex and base excision repair factors in mouse fibroblasts

Rajendra Prasad, Jason G. Williams, Esther W. Hou and Samuel H. Wilson*

Laboratory of Structural Biology, NIEHS, National Institutes of Health, 111 T.W. Alexander Drive, Research Triangle Park, NC 27709, USA

Received January 12, 2012; Revised August 21, 2012; Accepted September 5, 2012

ABSTRACT

During mammalian base excision repair (BER) of lesion-containing DNA, it is proposed that toxic strand-break intermediates generated throughout the pathway are sequestered and passed from one step to the next until repair is complete. This stepwise process is termed substrate channeling. A working model evaluated here is that a complex of BER factors may facilitate the BER process. FLAG-tagged DNA polymerase (pol) β was expressed in mouse fibroblasts carrying a deletion in the endogenous pol β gene, and the cell extract was subjected to an 'affinity-capture' procedure using anti-FLAG antibody. The pol β affinity-capture fraction (ACF) was found to contain several BER factors including polymerase-1, X-ray cross-complementing factor1-DNA ligase III and enzymes involved in processing 3′-blocked ends of BER intermediates, e.g. polynucleotide kinase and tyrosyl-DNA phosphodiesterase 1. In contrast, DNA glycosylases, apurinic/aprymidinic endonuclease 1 and flap endonuclease 1 and several other factors involved in BER were not present. Some of the BER factors in the pol β ACF were in a multi-protein complex as observed by sucrose gradient centrifugation. The pol β ACF was capable of substrate channeling for steps *in vitro* BER and was proficient in *in vitro* repair of substrates mimicking a 3′-blocked topoisomerase I covalent intermediate or an oxidative stress-induced 3′-blocked intermediate.

INTRODUCTION

Genomic DNA suffers damage from a variety of physical and chemical agents, resulting in base loss and multiple other lesions. Failure to accurately repair DNA lesions can lead to deleterious mutations, genomic instability or cell death. In higher eukaryotes, the DNA damage occurring in genes responsible for cell cycle regulation, growth control and DNA repair can lead to life-threatening disease and degeneration. To repair DNA damage, cells have multiple and overlapping DNA repair pathways that are essential for maintaining the integrity of genomic DNA. A major repair pathway protecting cells against single-base loss, single-strand breaks and base damage is known as base excision repair (BER). This repair pathway purifies genomic DNA of base and strand-break lesions arising from a wide variety of exogenous and endogenous sources, including environmental genotoxicants, methylating and oxidizing agents and other common exposures such as ionizing and ultraviolet irradiation (1–3).

A current working model for mammalian BER involves two sub-pathways: Single-nucleotide BER and long-patch BER. These sub-pathways are differentiated by repair patch size and the enzymes involved (4–8). For both BER sub-pathways, the initiating stage consists of modified base removal by a DNA glycosylase that hydrolyzes the N-glycosylic bond linking the damaged base to the sugar phosphate backbone (9–11). The resulting apurinic/apyrymidinic (AP) site intermediate is incised either 5′or 3′to the AP site sugar (12). In single-nucleotide BER, the DNA intermediate containing a single-nucleotide (1-nt) gap with 3′-OH and 5′-deoxyribose phosphate (dRP) groups at the margins is processed by replacement of the missing base and removal of the 5′-sugar phosphate by DNA polymerase (pol) β (13–17). The DNA backbone at the AP site also can be cleaved by another type of strand incision enzymatic activity, termed AP lyase (12,18). In this case, the strand is incised 3′ to the AP site by a β-elimination mechanism producing 3′-dRP and 5′-phosphate groups at the 1-nt gap margins. In some cases, the 3′-dRP is removed by δ-elimination leaving a 3′-phosphate blocking group. Traditionally, AP lyase activity was found associated with some of the oxidized base DNA glycosylases (19), and it also has been shown that pol β and poly(ADP-ribose) polymerase-1 (PARP-1) can recognize and incise the AP site via their AP lyase activities (20). After lyase incision, the 1-nt gap 3′-margin-blocking

*To whom correspondence should be addressed. Tel: +1 919 541 4701; Fax: +1 919 541 4724; Email: wilson5@niehs.nih.gov

group is removed by polynucleotide kinase (PNK) or AP endonuclease 1 (APE1), and the 1-nt gap is then filled by pol β (12,18–21). The final repair intermediate containing a nick is sealed by either DNA Ligase (Lig) I or III (22–24). The multiple steps after strand incision and margin trimming have been termed 'late stage' BER (12,25,26).

Many of the DNA transactions and proteins involved in the BER pathway are well characterized in mammalian systems. Multiple examples of protein–protein interactions among individual enzymes and cofactors of BER have been reported. These protein–protein interactions include X-ray cross-complementing factor1 (XRCC1) interactions with pol β, PARP-1, DNA Lig III (22,27) and aprataxin (28), among many others. Protein–protein interactions also have been reported between pol β and the following factors: high mobility group box 1 (HMGB1) (29), DNA Lig I (23), APE1 (30,31), proliferating cell nuclear antigen (PCNA) (32), PARP-1 (30,33), PNK (28), tyrosyl-DNA phosphodiesterase 1 (Tdp1) (34), nei-like-1 (NEIL1) and nei-like-2 (NEIL2) DNA glycosylases (18,35), heat shock protein 70 (36), p53 (37,38), Rad9-Rad1-Hus1 (9-1-1) (39–41) and the *adenomatous polyposis coli* protein, among others (42). Thus, it appears a wide range of interacting proteins can influence the BER pathway. Although pol β-mediated BER has been reconstituted *in vitro* using several of these interacting proteins, it is unclear in most cases as to the mechanism of how the protein–protein interactions influence BER. Therefore, to better understand underlying mechanisms of BER regulation, comprehensive study to understand and identify interacting BER factors is still necessary.

Many strand-break products of DNA transactions are cytotoxic. For example, the 5′-dRP group in the BER intermediate after APE1 strand incision is a cytotoxic lesion in mammalian cells resulting from stalled BER after DNA damage by methylating agents. Removal of the 5′-dRP group was found to be critical in cell sensitivity studies of BER *in vivo* (43): Fibroblasts from pol β null embryonic mice are hypersensitive to monofunctional DNA methylating agents, and persistence of the 5′-dRP group signals downstream events such as apoptosis and necrotic cell death (44). Furthermore, oxidized abasic sites introduced by free radicals and other reactive oxygen species render the abasic site sugar refractory to the β elimination required in the dRP lyase activity of pol β (45). In addition, DNA with base lesions, nicks or short gaps immediately opposite or adjacent to a topoisomerase 1 (top1) cleavage site are substrates for irreversible top1 cleavage, resulting in dead-end complexes with blocked 3′-ends (known as 'suicide or aborted complexes' (46). If unrepaired, the BER intermediates containing the intact AP site, 5′-dRP or various 3′-end blocking groups have cytotoxic and/or mutagenic consequences (43,47,48).

In the present study, we made use of an affinity-capture technique along with mass spectrometry to first isolate and then characterize a fraction representing an interactome of pol β (49,50). An octapeptide tag (FLAG) was added to the N-terminus of pol β. FLAG-tagged pol β was expressed in pol β null mouse fibroblasts, and the pol β 'affinity-capture fraction' (ACF) was isolated by anti-FLAG affinity chromatography. Proteins in the ACF were identified by mass spectrometry and confirmed by immunoblotting and enzymatic activity assays. Many of the components of the ACF were recognized BER factors, yet APE1 and the BER DNA glycosylases were not present. Interestingly, the ACF contained PNK and Tdp1 and was competent with BER substrates with blocked 3′-margins, such as the single-strand break mimicking the top1 covalent complex. The notion that a multi-protein complex of BER factors could facilitate the repair process is discussed.

MATERIALS AND METHODS

Materials

Synthetic oligodeoxyribonucleotides were from Oligos Etc., Inc. (Wilsonville, OR, USA) and The Midland Certified Reagent Co. (Midland, TX, USA). [α-^{32}P]dCTP and [α-^{32}P]3′-deoxyadenosine (Cordycepin) (3000 Ci/mmol) were from GE Healthcare (Piscataway, NJ, USA). [γ-^{32}P]ATP (7000 Ci/mmol) was from Biomedicals (Irvine, CA, USA). Optikinase and terminal deoxynucleotidyl transferase were from USB Corp. (Cleveland, OH, USA) and Fermentas Inc. (Hanover, MD, USA), respectively. Anti-pol β affinity purified monoclonal (18S) and anti-APE1 polyclonal antibodies have been described previously (23). Anti-DNA Lig III (1F3), anti-DNA Lig I (10H5) and anti-HMGB1 (HAP46.5) were from Genetex (San Antonio, TX, USA). Anti-PARP-1, anti-Ku70/Ku80 and anti-XRCC1 were from BD Biosciences PharMingen (San Jose, CA, USA) and Abcam (Cambridge, MA, USA), respectively. Anti-PCNA and anti-PNK (V20) were from Santa Cruz Biotechnology (Delaware, CA, USA). The secondary antibodies, anti-mouse immunoglobulin (IgG) (H+L) and goat anti-rabbit IgG (H+L) conjugated to affinity-purified horseradish peroxidase, were from Bio-Rad Laboratories (Hercules, CA, USA). Anti-FLAG agarose gel was from Sigma-Aldrich (St. Louis, MO, USA). Protease inhibitors complete cocktail (EDTA free) was from Roche Molecular Diagnostics Corp. (Indianapolis, IN, USA). Leupeptin, aprotinin and phenylmethylsulfonyl fluoride were from Calbiochem (La Jolla, CA, USA). The high molecular weight gel filtration kit that contained thyroglobulin (700 kDa), apoferritin (443 kDa), catalase (250 kDa) and aldolase (164 kDa) was from GE Healthcare (Piscataway, NJ, USA). Recombinant human pol β was overexpressed and purified as described previously (51). Human APE1, uracil DNA glycosylase (UDG) with 84 amino acids deleted from the amino terminus and DNA Lig I were purified as described previously (11,52,53).

5′- and 3′-end labeling for $NaBH_4$ cross-linking

Dephosphorylated 34-mer oligodeoxyribonucleotide (5′-CTGCAGCTGATGCGCUGTACGGATCCCCGGGTAC-3′) containing a uracil residue at position 16 was either 3′- or 5′-end labeled with terminal deoxynucleotidyl transferase and [α-^{32}P] Cordycepin or with Optikinase and [γ-^{32}P]ATP, respectively. The 34-mer (5′-GTACCCGGGGATCCGTACGGCGCATCAGCTGCAG-3′) template

was annealed with ^{32}P-labeled oligonucleotides by heating the solution at 90°C for 3 min and allowing the solution to slowly cool to 25°C. Unincorporated [α-^{32}P] Cordycepin or [γ-^{32}P]ATP was removed by using a MicroSpin™ G-25 column (GE Healthcare) using the manufacturer's suggested protocol.

UDG and APE1 treatment of DNA substrate

Typically, 400 nM DNA substrate was pretreated with 50 nM UDG in 50 mM HEPES, pH 7.4, 1 mM EDTA and 2 mM dithiothreitol (DTT). The reaction mixture was incubated for 20 min at 30°C. After this incubation, the reaction mixture was divided into two equal portions. One portion was supplemented with 10 mM $MgCl_2$ and 50 nM APE1 and incubated for 20 min at 37°C to generate incised AP site-containing DNA. Owing to the labile nature of the incised AP site-containing DNA, the DNA substrate was prepared just before performing the $NaBH_4$ trapping experiment.

$NaBH_4$ cross-linking

$NaBH_4$ cross-linking of PARP-1 was performed with 5′- or 3′-end ^{32}P-labeled DNA pre-treated with UDG or UDG and APE1 that contained the intact AP site or incised AP site, respectively, essentially as described previously (54). Briefly, the reaction mixture (10 μl) contained 50 mM HEPES, pH 7.4, 1 mM EDTA, 2 mM DTT, 200 nM ^{32}P-labeled duplex DNA, 100 or 200 nM purified PARP-1 and 5 mM $NaBH_4$. The reaction mixture was incubated for 60 min on ice. After incubation, the reaction was terminated by the addition of 10 μl of gel-loading dye. Nu-PAGE Bis-Tris gel and MOPS running buffer system were used to separate protein–DNA cross-linked complexes. A Typhoon PhosphorImager (GE Healthcare) was used for scanning the gels.

Isolation of the pol β ACF with anti-FLAG M2 affinity gel

Pol β null cells expressing FLAG-tagged pol β or pol β null cells (control) were washed twice with phosphate-buffered saline at room temperature, detached by scraping, pelleted by centrifugation and re-suspended in a lysis buffer (LB) (55) that contained 50 mM Tris-HCl, pH 7.5, 150 mM NaCl, 2 mM EGTA, 2 mM EDTA, 25 mM NaF, 25 mM β-glycerophosphate, 0.2% Triton X-100, 0.3% Nonidet P-40 and protease inhibitors cocktail. The cell suspension was then incubated on ice for 30 min. The resulting lysate was centrifuged at 14 000 rpm for 30 min at 4°C, and the clear supernatant fraction was transferred to another tube. The protein concentration of this extract was determined using the Bio-Rad protein assay, with bovine serum albumin as standard. For immunoprecipitation of FLAG-tagged pol β and its binding partners, ~40 mg of cell extract was mixed with ~400 μl of anti-FLAG M2 affinity gel, which was washed and pre-equilibrated with LB according to the manufacturer's instructions. The cell extract and anti-FLAG M2 affinity gel suspension were incubated with a gentle rotation for 4 h at 4°C. After this incubation, the resin was centrifuged at 3000 rpm for 30 s at 4°C. Supernatant fractions were carefully removed with a narrow-end pipette tip. The resin was washed four times with the LB, and this was followed by 10 washes with wash buffer (50 mM Tris-HCl, pH 7.4 and 150 mM NaCl), to remove all non-specific proteins. Then, FLAG-tagged bound pol β and its interacting proteins were eluted by competitive elution with 200 μl of a solution containing 100 μg/ml FLAG peptide in 50 mM Tris-HCl, pH 7.4, 150 mM NaCl. The elution step was repeated two times. All the eluted fractions were combined and referred as the ACF. This fraction was stored in small aliquots at −80°C.

Mass spectrometry

NanoLC-ESI-MS/MS analyses were performed using an Agilent 1100 nanoLC system on-line with an Agilent XCT Ultra ion trap mass spectrometer with the chip cube interface, and the details are described in the Supplementary data.

In vitro BER assay

The BER assay was performed in a final reaction mixture volume of 30 μl, as described previously (16,23). The BER reaction mixtures contained 50 mM HEPES, pH 7.5, 0.5 mM EDTA, 2 mM DTT, 20 mM KCl, 5 mM $MgCl_2$, 4 mM ATP, 5 mM phosphocreatine, 100 μg/ml phosphocreatine kinase, 0.5 mM NAD, 2.3 μM [α-^{32}P]dCTP (specific activity, 1×10^6 dpm/pmol) and 250 nM 35-base pair DNA with a uracil at position 15. In some cases, the reaction mixtures were also supplemented with 20 nM each UDG and APE1 and 200 nM DNA Lig I, as indicated in the figure legends. The repair reactions were then initiated by the addition of 30 μg extract or 6 μl ACF/control fraction, and the incubation was at 37°C. Aliquots (9 μl) were withdrawn at the indicated periods. The reaction was terminated by the addition of an equal volume of DNA gel-loading buffer (95% formamide, 20 mM EDTA, 0.02% bromophenol blue and 0.02% xylene cyanol). After incubation at 75°C for 2 min, the reaction products were separated by electrophoresis in a 16% polyacrylamide gel containing 8 M urea in 89 mM Tris-HCl, pH 8.8, 89 mM boric acid and 2 mM EDTA. A Typhoon PhosphorImager was used for gel scanning and imaging, and the data were analyzed by ImageQuant software.

Tdp1 activity assay with DNA substrate containing the 3′-phosphotyrosyl group

A 17-mer DNA oligonucleotide containing the 3′-phosphotyrosyl group was 5′-end labeled with Optikinase and [γ-^{32}P]ATP and then annealed to a 5′-phosphorylated 18-mer down-stream primer and 36-mer template duplex (Substrate 1). The reaction mixture (10 μl) containing 50 mM HEPES, pH 7.5, 0.5 mM EDTA, 2 mM DTT, 20 mM KCl, 100 nM ^{32}P-labeled duplex DNA with or without 5 mM $MgCl_2$, 5 mM EDTA or 20 μM dCTP was assembled on ice, as indicated in the figure legends. Reactions were initiated by the addition of 2 μl ACF and transferring the reaction mixtures to 37°C. After a 30-min incubation, the reactions

were stopped by the addition of an equal volume of DNA gel-loading buffer and heating at 75°C for 2 min. The reaction products were analyzed as mentioned earlier.

In vitro BER: assay with 3′-end blocked DNA substrates

Oligonucleotide duplex DNA containing the 3′-phosphotyrosyl group (Substrate 1) or the 3′-phosphate group (Substrate 2) in a gap were used for testing Tdp1 and PNK activities, respectively. *In vitro* BER reaction mixtures were in a final volume of 20 µl. The repair reaction mixture contained 50 mM HEPES, pH 7.5, 0.5 mM EDTA, 2 mM DTT, 20 mM KCl, 5 mM $MgCl_2$, 4 mM ATP, 5 mM phosphocreatine, 100 µg/ml phosphocreatine kinase, 0.5 mM NAD, 2.3 µM [α-^{32}P]dCTP (specific activity, 1×10^6 dpm/pmol) and 250 nM DNA substrate. Reaction mixtures included ACF (2 µl/mixture), pol β (20 nM), or DNA Lig I (250 nM), as indicated in the figure legends. Incubation was at 37°C for 20 and 40 min. Aliquots (9 µl) were withdrawn at the indicated periods. The reaction was terminated by the addition of an equal volume (9 µl) of DNA gel-loading buffer. After incubation at 75°C for 2 min, the reaction products were analyzed as mentioned earlier.

In vitro BER: substrate channeling by the ACF

BER substrate channeling experiments in the presence of a trap (1-nt gapped DNA, BER intermediate that was able to sequester free BER enzymes) were performed essentially as described (26). Briefly, to study combined gap-filling DNA synthesis, 5′-dRP lyase and ligation reactions in the presence of a DNA trap, a reaction mixture containing 50 mM HEPES, pH 7.5, 20 mM KCl, 2 mM DTT, 4 mM ATP, 0.5 mM NAD, 0.5 mM EDTA, 20 nM UDG/APE1 pre-treated gapped DNA or 10 µM unlabeled DNA trap and the ACF (2 µl/10 µl final reaction volume) was assembled on ice. The reaction was initiated by transferring the reaction mixture to 30°C and adding a mixture of 10 µM unlabeled DNA trap or 20 nM UDG/APE1 pre-treated gapped DNA substrate, 2.6 µM [α-^{32}P]dCTP and 5 mM $MgCl_2$. Immediately (within 5–10 s of incubation), the reaction was terminated by addition of an equal volume of gel-loading dye solution. Then, after incubation at 75°C for 2 min, the reaction products were separated by electrophoresis. Some of the reaction mixtures were supplemented with 200 nM DNA Lig I or DNA Lig III, as indicated.

Poly(ADP-ribosyl)ation assay

The Poly(ADP-ribosyl)ation (PARylation) reaction mixture was assembled essentially as described previously (20). Briefly, the reaction mixture (10 µl) containing 50 mM HEPES-KOH, pH 7.5, 0.5 mM EDTA, 20 mM KCl, 2 mM DTT, 5 mM $MgCl_2$, 100 nM double-hairpin DNA (UDG- or UDG/APE1- pre-treated) and 100 µM [^{32}P]NAD^+ was assembled on ice. The PARylation reaction was then initiated by the addition of ACF (2 µl) and incubation at 37°C for the indicated times. Reactions were terminated by the addition of 10 µl SDS-PAGE buffer and heating for 5 min at 95°C. The reaction product was analyzed by Nu-PAGE 4–12% Bis-Tris mini-gel (Life Technologies, Grand Island, NY, USA) with subsequent phosphorimaging.

Immunoblotting

The isolated ACF/control fraction (150 µl) was precipitated with 10% TCA on ice for 30 min, and the precipitates were collected by centrifugation. Precipitates were then re-suspended in 10 µl of 1 M Tris-HCl, pH 8.0 and 20 µl SDS-PAGE sample buffer. Extracts (20 µg) from pol β null cells or FLAG-tagged pol β expressing cells were separated by Nu-PAGE 4–12% Bis-Tris mini-gel and transferred onto nitrocellulose membranes. The membranes were incubated with 5% non-fat dry milk in Tris-buffered saline containing 0.1% (v/v) Tween 20 and probed with antibody either to pol β (18S), DNA Lig III, PARP-1, XRCC1, PCNA, HMGB1, APE1, DNA Lig I, PNK or Ku80, as indicated in the figure legends. Goat anti-rabbit or goat anti-mouse IgG conjugated to horseradish peroxidase (1:10 000 dilution) was used as secondary antibody, and immobilized horseradish peroxidase activity was detected by enhanced chemiluminescence. These membranes were stripped by incubation in Restore Western Blot Stripping Buffer (Thermo Scientific, Rockford, IL, USA) for 30 min at room temperature, followed by two washes with Tris-buffered saline containing Tween 20. Then, the membrane was used for probing with another antibody, as mentioned earlier.

Sucrose gradient centrifugation

The ACF (150 µl) eluted from the anti-FLAG agarose gel or the cell extract was layered onto a 10–40 % sucrose density gradient (SDG) prepared in 50 mM Tris-HCl, pH 7.4, 150 mM NaCl. Centrifugation was performed in a Beckman SW55 rotor either at 45 000 rpm at 4°C for 15 h or 45 000 rpm at 4°C for 13.5 h. Fractions, ~80 µl (three drops), were collected from the bottom of the tube connected through a peristaltic pump. A parallel gradient under similar conditions was calibrated with 120 µg each of thyroglobulin (700 kDa), apoferritin (443 kDa), catalase (250 kDa), aldolase (164 kDa) and pol β (39 kDa). The identity and position of these marker proteins were verified by Coomassie blue staining after SDS-PAGE. The molecular mass of the ACF complex was determined from the linear plot developed by plotting the molecular mass (kDa) of these marker proteins against the peak fractions as they appeared in the gradient.

RESULTS

Isolation of the Pol β ACF and protein identification

The availability of immunoaffinity-capture technology enabled us to isolate a multi-protein ACF using pol β as 'bait'. The ACF was isolated from mouse fibroblasts in log phase culture using cell extract prepared under native conditions. This method involved fusion of the FLAG epitope at the N-terminus of pol β in an expression vector and the stable transfection of pol β null cells, allowing expression of 'FLAG-tagged-pol β'· Pol β null cells were chosen to

Table 1. Summary of mass spectrometry analyses of pol β-interacting proteins (seven independent experiments)

Known BER enzymes/ factors found	Known BER enzymes/factors NOT found	Other proteins routinely found
Found in abundance in all experiments		
Pol β	DNA glycosylases	Ku70/80
DNA Lig III	APE1	Hdac6
XRCC1	FEN1	Histones 1, 3, 2A, B
PARP-1	HMGB1	Rpl12
PNK		PPP1R12A
Tdp-1		IMPDH2
RPA		
Found as a minor component in some experiments		
Aprataxin		
PARP-2		
Y-box protein 1		
Heat shock protein 70		
Ribosomal protein S3		

PPP1R12A and IMPDH2 denote protein phosphate 1 regulatory (inhibitor) subunit 12 and inosine 5′-monophosphate dehydogenase 2, respectively.

avoid competition by endogenous pol β. The expression level of this tagged form of pol β was assessed by immunoblotting and found to be somewhat higher (3-fold) than the level in wild-type cells (Supplementary Figure S1).

We used a mild procedure for extract preparation including an extraction buffer at physiological ionic strength and pH. Extract from pol β null cells was used as the negative control. This extract and extract from FLAG-tagged pol β expressing cells were incubated with anti-FLAG affinity gel (Supplementary Figure S2). After the incubation, non-specific proteins were removed by extensive washing, and proteins bound to the affinity gel were batch eluted with FLAG peptide. These proteins isolated from the pol β expressing cells were termed the 'ACF'. The proteins in the ACF were resolved by SDS-PAGE and then subjected to in-gel trypsin digestion and mass spectrometry. A database search was used to identify the proteins. All proteins corresponding to peptides observed with the pol β null negative control sample were considered as non-specific and used to differentiate the specific affinity-capture proteins. This procedure was repeated a number of times with independently derived extract samples; similar results were consistently obtained (Table 1 and Supplementary Tables S1–S3). Finally, an identical affinity-capture experiment was conducted with mouse fibroblasts cells that had been treated with methyl methanesulfonate (45). The results with the ACF from these cells were similar to those obtained with extracts from the untreated cells (Supplementary Table S3).

Five well-known BER factors, in addition to pol β, were consistently found in the ACF (Table 1). The presence of PARP-1, XRCC1 and DNA Lig III was confirmed by immunoblotting (Supplementary Figure S3A). In other experiments, the presence of Ku80, PNK and Tdp-1 in the ACF was also confirmed (Supplementary Figure S3C and data not shown, respectively). Replication protein A (RPA) also was observed in the ACF and is considered as a BER factor (56).

In addition to these proteins, other proteins implicated in BER were observed in some experiments (Table 1), including aprataxin, PARP-2, Y-box binding protein-1, ribosomal protein S3 and heat shock protein 70. As summarized in Table 1, many known BER proteins were not found in the ACF, including the DNA glycosylases, APE1, flap endonuclease 1 and HMGB1 (Table 1 and Supplementary Figure S3B). Interestingly, a number of proteins that have unknown BER functions were observed in the ACF in all experiments and with high confidence scores (Table 1 and Supplementary Tables S1–S3). These proteins included Ku antigen; histone deacetylase 6; histone proteins H1, H3, H2A and H2B; ribosomal protein L12; protein phosphatase 1 regulatory subunit 12 and inosine 5′-phosphate dehydrogenase 2. The functional significance of these proteins in the ACF remains to be investigated.

Properties of the ACF

Assessment of DNA contamination

We conducted experiments to evaluate the possibility of DNA contamination in the ACF. First, in experiments where ethidium bromide was added to the cell extracts before the affinity-capture procedure, we obtained results very similar to those without ethidium bromide treatment, suggesting that DNA contamination was not an issue in the results (Supplementary Table S2). Next, the absence of DNA in the ACF was confirmed by biochemical assays: (i) A 5′-end labeling-based DNA assay, using T4 PNK and [γ-^{32}P]ATP, failed to reveal DNA in the ACF (Supplementary Figure S4); and (ii) self-PARylation of PARP-1 activity in the ACF was evaluated for its dependence on added nicked DNA. PARP-1 activity of the ACF was negative unless nicked DNA was added to the reaction mixture (see Figure 3B, lane 2). Taken together, these results suggest that the ACF was free of DNA contamination.

BER capacity of the ACF

We first confirmed the *in vitro* BER status of the ACF. In the experiments shown in Figure 1A, uracil-DNA was used as substrate with or without treatment with purified UDG and APE1. The ACF failed to support uracil-DNA BER in the absence of UDG and APE1 (Figure 1A, lanes 1–3). But, ACF showed BER activity when the reaction mixtures contained these enzymes (Figure 1A, lanes 4–6). The ACF was partially deficient in DNA ligase activity, despite the presence of DNA Lig III (Table 1). This deficiency could be overcomed by including purified DNA Lig I in the reaction mixture (Figure 1A, lanes 7–9). A control fraction isolated from pol β null cells failed to support BER activity (Supplementary Figure S5).

BER substrate channeling and the ACF

We had shown previously that BER steps can be processive in reaction mixtures with purified BER

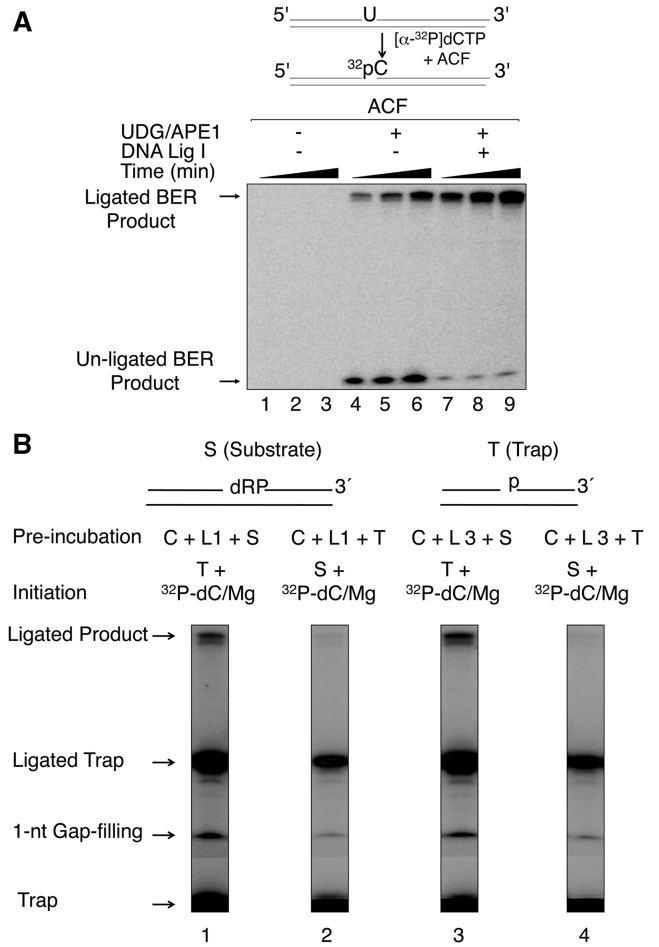

Figure 1. BER capacity of the ACF. Schematic representation of the substrate and the reaction scheme is shown at the top. The reaction conditions and product analysis were as described under Materials and Methods. The repair reaction mixture (30 µl) was assembled on ice that contained 50 mM HEPES, pH 7.5, 0.5 mM EDTA, 2 mM DTT, 20 mM KCl, 5 mM $MgCl_2$, 4 mM ATP, 5 mM phosphocreatine, 100 µg/ml phosphocreatine kinase, 0.5 mM NAD, 2.3 mM [α-^{32}P]dCTP (specific activity, 1×10^6 dpm/pmol) and 250 nM 35-base pair DNA with a uracil at position 15. Repair reactions, UDG/APE untreated (lanes 1 and 3) or treated (lanes 4–9) were initiated by the addition of 6 µl the ACF and incubation at 37°C. Aliquots (9 µl) were withdrawn at 5, 10 and 20 min. The reaction mixtures in lanes 7–9 were supplemented with 200 nM DNA Lig I, as indicated. The repair reaction was terminated by the addition of an equal volume (9 µl) of DNA gel-loading buffer. After incubation at 75°C for 2 min, the reaction products were separated by electrophoresis in a 16% polyacrylamide gel containing 8 M urea. A Typhoon PhosphorImager was used for gel scanning and imaging. The positions of un-ligated and ligated BER products are indicated. (**B**) BER substrate channeling in the ACF. Schematic representations of UDG/APE1-treated DNA substrate (S) and the DNA trap (T) are illustrated above the phosphorimage of the gels. The reaction mixture containing the pre-treated DNA substrate (S) or trap DNA (T), with or without DNA Lig I (L1) or DNA Lig III (L3) and the ACF (C) was assembled on ice. The reaction was initiated by temperature jump and the addition a mixture of [α-^{32}P]dCTP, $MgCl_2$, ATP and DNA trap (lanes 1 and 3) or [α-^{32}P]dCTP, $MgCl_2$, ATP and DNA substrate (lanes 2 and 4), as indicated at the top of each lane. Samples were withdrawn at 10 s and then analyzed as in (**A**). The positions of the 1-nt gap-filling product, ligated BER product, free trap and the ligated trap are indicated. A minor amount of gap-filling product was observed in the presence of the trap.

factors (26) such that BER intermediates are channeled from one step to the next, forming complete BER products in the presence of a trap (a 1-nt gapped DNA, BER intermediate, that was able to sequester free BER enzymes). We examined whether the ACF was similarly capable of conducting BER in the presence of a trap. The reaction mixtures were assembled on ice, and the reactions were initiated by transferring the tubes to 30°C and adding a mixture of DNA ligase, [α-^{32}P]dCTP, $MgCl_2$ and ~500-fold excess of DNA trap (Figure 1B). In a parallel set of reaction mixtures, used as a negative control, the ACF was first pre-incubated with the DNA trap, and then the reactions were initiated by adding the mixture of DNA substrate, DNA ligase, [α-^{32}P]dCTP and $MgCl_2$. The results revealed that when the ACF was pre-incubated with the substrate, the complete ligated BER product was observed (Figure 1B, lanes 1 and 3). When the ACF was first pre-incubated with the trap, repair products were not observed (Figure 1B, lanes 2 and 4). These results indicated that the BER substrate was subjected to dRP lyase and gap-filling and then passed on to the ligation step in a processive fashion. Thus, the product formed represented a single-turnover reaction for the ACF components bound to the substrate DNA during the pre-incubation.

Affinity-capture fraction and a complex of BER factors

Detection of BER factors in a complex

To assess whether BER factors in the ACF could be found in a multi-protein complex, we performed SDG sedimentation analyses. After centrifugation, fractions were collected and proteins were separated by SDS-PAGE, transferred to a nitrocellulose membrane and probed with monoclonal antibody against pol β. The monomeric form of pol β was observed and centered at fraction 52; however, a large portion of pol β sedimented in a higher mass range of the SDG centered at fraction 3 (Figure 2A). As this fraction was close to the bottom of the gradient, we adjusted the sedimentation conditions such that this pol β peak was now centered at fractions 14–18 (Figure 2B); the molecular mass of the protein complex migrating in these fractions was ~900 kDa. Pol β also was observer in fraction 2 near the bottom of the gradient and in fractions corresponding to lower molecular mass complexes (fraction 20–30).

Having observed pol β in higher molecular mass range fractions consistent with a complex with other proteins, the peak fractions were pooled and analyzed for other BER factors by immunoblotting with antibody against pol β, PARP-1, DNA Lig III and XRCC1. These proteins were found to be present along with pol β (Supplementary Figure S7), indicating that the ACF contained a complex of pol β and several other BER factors.

Complexes of BER factor in cell extracts

Having observed a complex of BER factors in the ACF, we wished to confirm the presence of a similar complex in the initial mouse fibroblasts cell extract. SDG sedimentation analyses were performed with the initial cell extract that was used for isolation of the ACF

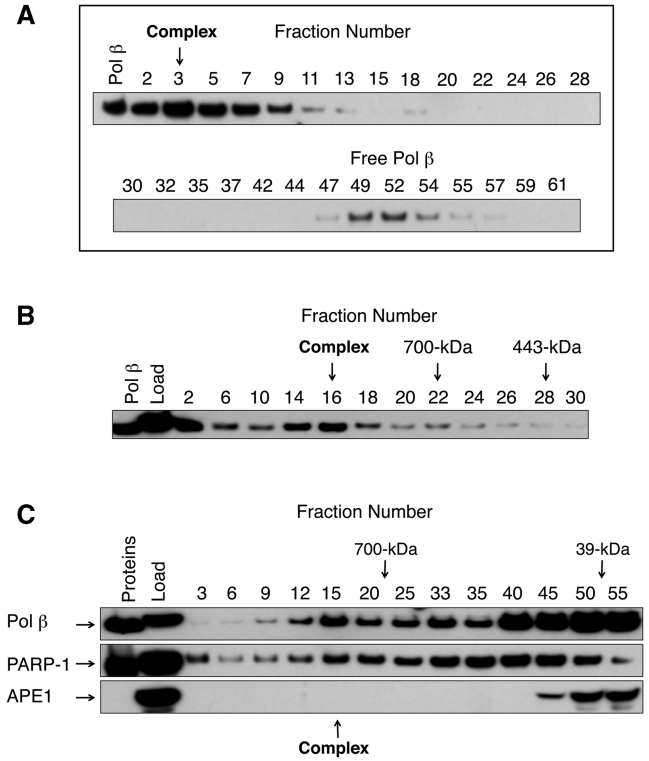

Figure 2. Assessment of BER multi-protein complex by sucrose gradient sedimentation. (**A**) Evidence of a multi-protein complex in the ACF. The ACF (150 µl) eluted from the anti-FLAG affinity gel was layerd on a 10–14% SDG, and the centrifugation was performed at 50 000 rpm at 4°C for 15 h (A) or at 45 000 rpm at 4°C for 13.5 h (**B**) as described under Materials and Methods. The indicated fractions 2 through 61 and purified pol β (positive controls) were separated by SDS-PAGE, transferred to a nitrocellulose membrane and probed with an antibody against pol β. Fraction numbers and the relative positions of the complex and free pol β in the SDG are indicated. (B) As the complex was close to the bottom of the gradient, the SDG analysis of the ACF was repeated under modified sedimentation conditions such that the complex centered around fractions 14-18. Analysis of fractions 2 though 30 was shown. Fraction numbers, the relative positions of the marker proteins and the complex are indicated. Markers for caliberation are shown in Supplementary Figure S6. (**C**) Evidence of a multi-protein complex in the cell extract. Whole cell extract (150 µl, 14 mg/ml) was analyzed by SDG under similar conditions as in 2B. After centrifugation, fractions were collected and the indicated fractions (12 µl each) 3 through 55, along with 40 µg of the loading sample (load) and purified proteins as positive controls, were separated by SDS-PAGE, transferred to a nitrocellulose membrane and probed with either anti-pol β, anti-PARP-1 or anti-APE1· The fraction number, approximate positions of the marker proteins and the complex are indicated.

(Figure 2C). After centrifugation, fractions were collected, and the indicated fractions along with the loading sample and purified proteins were separated by SDS-PAGE; proteins were transferred to a nitrocellulose membrane and probed for two markers of the complex, pol β and PARP-1, and for APE1 as a negative control Figure 2C). As expected, the monomeric form of pol β sedimented in fractions 40–55 corresponding to the region of the gradient where lower molecular mass proteins are found (Figure 2C). A portion of the pol β in the gradient also was observed in a peak centered at fraction 15. This region of the gradient coincided with the region where the multi-protein complex was observed in Figure 2B. Interestingly, pol β also was found in lower molecular mass complexes, consistent with previous results with bovine testis nuclear extract (23). When the same membrane was probed with anti-PARP-1 antibody, PARP-1 was observed in multiple regions of the gradient and some coincided with pol β. However, PARP-1 exhibited a different sedimentation pattern than pol β (Figure 2C). APE1 was not detected in any of the higher molecular mass regions of the gradient; only fractions in the lower mass region of the gradient were positive (Figure 2C). The absence of APE1 in fractions corresponding to the ACF complex was consistent with the results of mass spectrometry and immunoblotting analyses of the ACF described earlier. Finally, we repeated the SDG sedimentation analysis with extract from normal wild-type mouse fibroblasts and probed for pol β as a marker for BER complexes. The pattern of pol β sedimentation was similar to that observed with the FLAG-tagged pol β expressing extract (Supplementary Figure S8).

PARP-1 in the ACF and its recognition of the AP site-containing BER intermediate

It is known that purified PARP-1 can interact with the AP site in a substrate DNA (20,30,57). As the PARP-1 in the ACF was also expected to recognize an AP site-containing BER intermediate, it is possible this enzyme could direct ACF components to the intermediate. To consider this, we first confirmed conditions for studying PARP-1 binding to the intact AP site. Covalent cross-linking of PARP-1 to the AP site Schiff base intermediate was assessed (Figure 3A). The substrate strand containing a uracil residue at position 16 was labeled at either the 3′- or 5′-end. Before incubation with purified PARP-1, substrates were treated with UDG alone (intact AP site) (lanes 1, 2, 5 and 6) or UDG plus APE (incised AP site) (Figure 3A, lanes 3, 4, 7 and 8). The results revealed that PARP-1 was cross-linked to the intact AP site-containing strand, as the cross-linked product would not be detected if the strand had been incised, as illustrated here in the control incubation where the AP site was pre-incised with APE1 (Figure 3A, lanes 3 and 4). These results confirmed PARP-1 cross-linking to the intact AP site-containing strand.

We next examined PARP-1 in the ACF for its recognition of AP site-containing DNA using a self-PARylation assay. The PARylation reaction mixtures, containing the ACF, [^{32}P]NAD^{+} and double-hairpin DNA with either an intact AP site or incised AP site, were assembled. Self-PARylation of PARP-1 was observed with either type of DNA, i.e. carrying the intact or incised AP site (Figure 3B), and there was no significant difference in the amount of PAR formed with the two types of DNA (Figure 3B). PARylation was not observed in the absence of the ACF, as expected (Figure 3B, lane 1) or in the reaction mixture without UDG (Figure 3B, lane 2). The verification of PARP-1 in the ACF was determined by immunoblotting (Figure 3C). The results confirmed that PARP-1 in the ACF was active for poly(ADP-ribose)

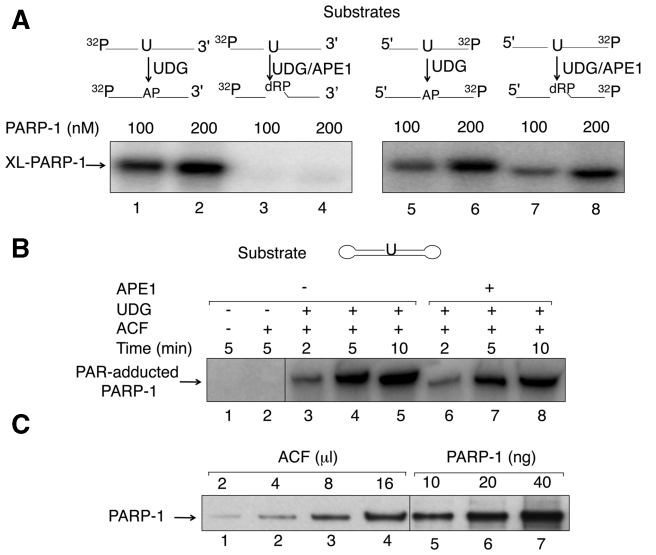

Figure 3. Binding of PARP-1 to the intact AP site. (**A**) Schematic representations of DNA probes are shown at the top. The term AP illustrates the presence of the AP site in the intact DNA strand, whereas the term dRP illustrates the presence of 5′-deoxyribose phosphate in the incised DNA strand. The binding of PARP-1 to the intact AP site was addressed by cross-linking after $NaBH_4$ reduction of PARP-1 and the AP site Schiff base intermediate. The substrate strand containing the uracil (U) residue was ^{32}P-labeled at the 5′-end or the 3′-end, as shown in the schematic of DNA probes at the top of phosphorimages. Both substrates were treated with UDG (lanes 1, 2, 5 and 6) or UDG plus APE1 (lanes 3, 4, 7 and 8) before incubation with purified PARP-1 (100 nM, lanes 1, 3, 5 and 7 or 200 nM, lanes 2, 4, 6 and 8). Reaction conditions and products analyses were as described under Materials and Methods. (**B**) PARylation of PARP-1 in the ACF. Schematic representation of the double-hairpin DNA substrate is shown at the top. The substrate was pre-treated with UDG (lanes 3–5) or UDG plus APE1 (lanes 6–8) as indicated. Lanes 1 and 2 represent controls without UDG. The PARylation reaction mixtures containing 50 mM HEPES-KOH, pH 7.5, 0.5 mM EDTA, 20 mM KCl, 2 mM DTT, 5 mM $MgCl_2$, 100 nM double-hairpin DNA and 100 μM [^{32}P]NAD^+ were assembled on ice. Reactions (lanes 2–8) were initiated by the addition of 2 μl ACF and the incubation at 37°C for 2, 5 and 10 min, as indicated. Reactions were terminated by addition of 10 μl SDS-PAGE buffer and heating for 5 min at 95°C. The reaction mixtures were analyzed by 4–12% SDS-PAGE with subsequent phosphorimaging. The position of PAR-adducted PARP-1 is indicated. (**C**) Verification and quantification of PARP-1 in ACF performed as in Figure 2. The amount of ACF (μl) and PARP-1 (ng), used as standard, is shown at the top. Increasing amounts of ACF, lanes 1–4 and increasing amounts of PARP-1, lanes 5–7 are shown. The concentration of PARP-1 in the ACF was ~0.6 ng/μl.

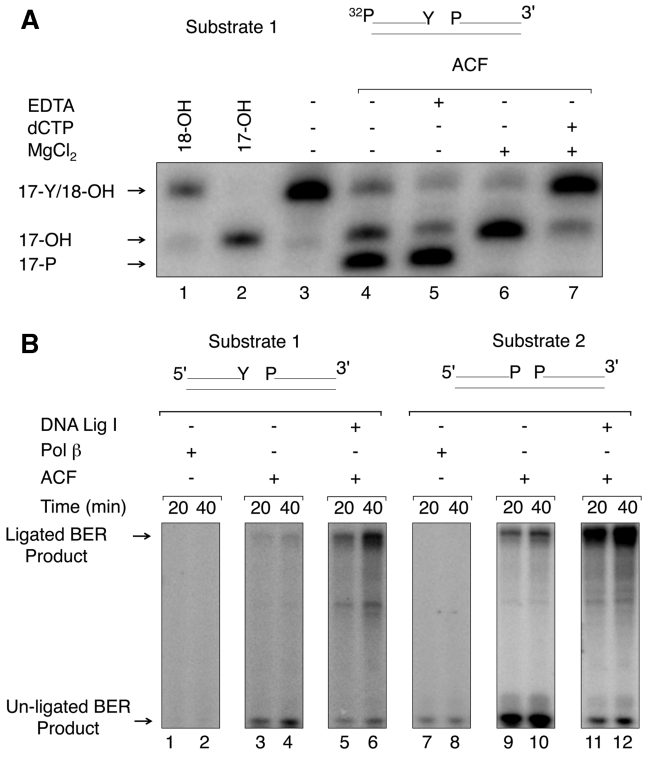

Figure 4. Repair of 3′-end blocked substrates by the complex. Schematic representation of the substrates is shown at the top of the phosphorimages. Substrate 1 represents the abortive top1-induced DNA strand break, whereas Substrate 2 represents the product of Tdp1 or an oxidative damaged-induced single-strand break with 3′-phosphate and 5′-phosphate margins in a 1-nt gapped DNA. (**A**) Tdp1 and PNK activities were evaluated using Substrate 1. The reaction mixtures contained the ^{32}P-labeled 17-Y substrate that was treated with ACF either in the absence (lanes 4 and 5) or in the presence (lanes 6 and 7) of $MgCl_2$ for 30 min. Lanes 1–3 illustrate DNA markers, 18-mer, 17-mer and Tdp1 substrate, respectively; lane 7 also contained 20 μM dCTP. Reactions were stopped by the addition of an equal volume of DNA gel-loading buffer. The reaction products were separated and analyzed as in Figure 1. The positions of 18-Y/18-OH, 17-OH and 17-P DNA were illustrated. (**B**) Schematic representation of the substrates is shown at the top. BER reaction was performed with the ACF and purified proteins. BER capacity of the ACF was evaluated using 3′-end blocked substrates by measuring incorporation of [α-^{32}P]dCMP as a function of incubation time and different components in the reaction. Reaction conditions and product analysis were as described under Materials and Methods. DNA substrate (250 nM) was mixed with (+) or without (−) the ACF (2 μl/10 μl reaction volume), pol β (20 nM) or DNA Lig I (250 nM), as indicated. Incubation was at 37°C for 20 and 40 min. Reaction products were analyzed as in Figure 1. The positions of un-ligated and ligated BER products are indicated.

synthesis and was able to recognize the intact AP site in a substrate DNA.

Repair of 3′-end blocked BER substrates by the ACF

We confirmed Tdp1 and PNK activities of the ACF using a 5′- ^{32}P-labeled substrate with a 3′-phosphotyrosine group (Figure 4A, Substrate 1). In the 3′-end unblocking process, Tdp1 cleavage of the bond between the 3′-phosphate and O4 of tyrosine generates the 3′-phosphate containing intermediate (17-P) that can be processed by PNK to the 3′-OH containing intermediate (17-OH). It is known that Tdp1 activity does not require a divalent metal ion, whereas PNK activity does. In the absence of added metal ion, the ACF primarily produced the 3′-phosphate containing Tdp1 product; however, a small amount of dephosphorylated 17-OH also was produced (Figure 4A, lane 4). Including EDTA to the reaction mixture resulted in a slight stimulation of 17-P formation and a reduction in 17-OH formation (Figure 4A, lane 5). Addition of $MgCl_2$ to the reaction mixture resulted in accumulation of the PNK product, 17-OH (Figure 4A, lane 6), owing to conversion of the 17-P Tdp1 product. When the reaction mixture was further supplemented with dCTP, the 17-OH molecule was extended to the 18-OH gap-filling polymerase product (Figure 4A, lane 7). These results were

indicative of Tdp1 activity, PNK activity and pol β activity in the ACF; in the presence of dNTP and $MgCl_2$, most of the initial 17-Y Tdp1 substrate was converted to the 18-OH polymerase product.

Next, the capacity of the ACF to conduct BER with two 3′-margin-blocked 1-nt gapped substrates was assessed. The substrates were chosen to mimic the abortive top1-induced strand break (Figure 4B, Substrate 1) and the oxidative damage-induced 1-nt gap with a 3′-phosphate (Figure 4B, Substrate 2). Purified pol β alone failed to incorporate significant radiolabeled dCMP into the gap with the 3′-blocked substrates, as expected (Figure 4B, lanes 1, 2, 7 and 8). When these substrates were incubated with the ACF, gap-filling synthesis with labeled dCMP was evident (Figure 4B, lanes 3, 4, 9 and 10). Most of the un-ligated BER product (intermediate) was converted to ligated BER product when the reaction mixtures were supplemented with DNA ligase I (Figure 4B, lanes 5, 6, 11 and 12). These results confirmed that the Tdp1, PNK and pol β activities in the ACF were capable of incising the 3′-phosphotyrosyl bond and producing substrate for DNA ligase·.

DISCUSSION

In this report, we described proteomics analysis of the pol β-interactome, identifying numerous interacting proteins through affinity-capture with FLAG-tagged pol β as bait. Proteins consistently found in the pol β ACF included the five well-known BER factors PARP-1, XRCC1, DNA Lig III, Tdp1 and PNK, and BER properties of several of these enzymes were evaluated here. Ku antigen and RPA also were observed in the ACF, but these proteins were not further evaluated here. A role of RPA in BER has been reported (56), but such a role for Ku antigen is unclear. The ACF contained a multi-protein complex as revealed by sucrose gradient centrifugation analyses. The complex sedimented at ~900 kDa, and the presence of some of the BER factors including pol β, PARP-1, XRCC1 and DNA Lig III was confirmed by immunoblotting. Interestingly, the important 'early phase' BER factors, such as DNA glycosylases and APE1, were not found in the ACF. Another interesting point was that the ACF contained enzymes for repair of 3′-blocked margins in BER intermediates. Thus, the ACF was proficient for *in vitro* BER of 3′-margin-blocked BER substrates (Figure 4) and 5′-margin-blocked (i.e. the 5′-dRP group) BER substrates (Figure 1A). The ACF BER activity with 5′-dRP-containing substrate exhibited substrate channeling, and it is reasonable to suggest that this may be facilitated by the multi-protein complex. Similarly, processing of the 3′-margin-blocked BER substrates was carried to completion by the ACF, with regard to the Tdp1, PNK and pol β activities (Figure 4). Understanding the precise mechanism of coordination of these multiple enzymatic steps will require further study.

Processing of BER intermediates with gaps and blocked margins is important to consider. These intermediates arise *in vivo* after numerous chemical and physical insults. For example, gaps with 3′-phosphate and 5′-hydroxyl groups are common products of radiochemical damage, and 3′-margin blocked BER intermediates are products of reactive oxygen species-mediated base oxidation. These BER intermediates with blocked margins are unable to serve as substrates for DNA polymerase and DNA ligase activities and, if not repaired, will lead to persistent single-strand breaks, replication mediated double-strand breaks, recombination and cell death. It is interesting that the 3′-phosphate and 5′-hydroxyl blocking lesions are repaired by the bifunctional enzyme PNK. This enzyme facilitates repair by phosphorylating the 5′-OH group and/or dephosphorylating the 3′-phosphate group at the margins of DNA gaps (58,59). XRCC1 facilitates PNK activities involving a direct protein–protein interaction (60).

Another type of 3′-margin blocked BER intermediate evaluated here was the top1 aborted complex that arises spontaneously or owing to DNA lesions proximal to top1 recognition sites, including base damage, base mismatches, abasic sites, ribonucleotides and DNA nicks. The top1 covalent DNA complex also is produced by anti-cancer drugs such as camptothecin, an inhibitor of the top1 re-ligation activity (46,61–63). The top1 covalent complex is repaired by proteolysis of top1 along with gap margin trimming by Tdp1. Tdp1 catalyzes the step of removal of the top1 tyrosine linked to the O3′ in the gap by hydrolyzing the covalent phosphotyrosyl bond between a top1 tyrosine residue and the O3′-phosphate group (64–66). The presence of Tdp1 and PNK (67) in the pol β ACF identified here is consistent with pol β-mediated BER of such 3′-margin top1 blocked BER intermediates. Nevertheless, it is also evident that the Tdp1 and PNK activities themselves must be carefully regulated, as PNK is expected to act on the Tdp1 product.

The complex isolated in the ACF contained the major DNA damage surveillance protein PARP-1, and repair events after loss of a damaged base could be mediated by the interaction of PARP-1 with intact AP site-containing DNA or incised AP site-DNA. Previous results had shown that PARP-1 is able to recognize AP sites via Schiff base formation (20), and we made use of the interaction of PARP-1 with intact and incised AP site-DNA to characterize PARP-1 in the ACF. PARP-1 in the ACF was found to be self-PARylated in reaction mixtures with AP site DNA (Figure 3), confirming the capacity of the complex-borne PARP-1 to interact with this lesion-containing DNA and to conduct PAR or poly(ADP-ribose) synthesis.

A current working model of mammalian BER highlights the role of XRCC1 as a scaffolding protein that interacts with multiple BER enzymes, including pol β, and facilitating recruitment of BER enzymes at lesion sites during BER (22,23,34,68–71). XRCC1 is required for pol β recruitment at laser-induced lesion sites in imaging experiments (70), and XRCC1 is known to facilitate PNK activities through a direct protein–protein interaction (60). Interestingly, both XRCC1 and PNK have been associated with BER defects in neurons (61,63), and Tdp1 has been associated with the neurodegeneration disease, spinocerebellar ataxia (72). In addition to these XRCC1 interactions, many other

BER factor protein–protein interactions have been reported (23,34,68–70,73–76). These include pol β interactions with early stage BER enzymes, such as the NEIL1 and NEIL2 DNA glycosylases (12,18,35) and APE1 (31,77). The failure to observe these factors in the ACF reported here was interesting. Similarly, the long patch BER factors flap endonuclease 1 and HMGB1 were not found in the ACF, even though protein–protein interaction between HMGB1 and pol β is known (29). One possibility is that some of these protein–protein interactions were not strong enough to survive the extensive affinity-capture washing protocol used here for isolation of the ACF. In addition, some of the BER factors, such as APE1, require a BER DNA substrate to interact stably (77) with pol β, and the ACF did not contain DNA.·

Our present results demonstrated that a pre-formed complex of BER factors is present in mouse fibroblasts, and no detectable change in the components of this complex was observed on methyl methanesulfonate treatment of these cells. The existence of the complex was demonstrated by SDG analyses, both with the ACF and the cell extract, and a complex of similar size was also observed in the wild-type cell extract. A consideration is that multi-protein BER complexes containing various enzymes and cofactors had been reported previously in mammalian systems (23,70). In most cases, these multi-protein complexes were isolated under different conditions (23,70) than those used here, and in most of these reports, the complexes were found to contain early stage BER factors and pol β (70 and S. Mitra, personal communication). One example of this was the complex previously isolated from bovine testis in this laboratory (23). This ~180-kDa complex was isolated after high-salt extraction of an isolated nuclear fraction, and evaluation revealed stable interaction between pol β and DNA ligase I and other factors sufficient for complete *in vitro* BER of a uracil-DNA substrate, including uracil-DNA glycosylase. Thus, the mouse fibroblasts derived ~900-kDa complex described in the present study differ in several respects from the bovine testis derived ~180-kDa complex. The mouse complex lacks DNA glycosylases and substantial DNA ligase I, but contains XRCC1 and DNA ligase III, along with PARP-1, and is much larger than the bovine complex. Overall, the results suggest the possibility of several distinct types of multi-protein complexes involved in BER and single-strand break repair, as previously discussed (23). The presence of pol β-containing complexes smaller than the ~900-kDa complex observed in the SDG analyses of extracts reported here is consistent with this idea (Figure 2 and Supplementary Figure S8).

It is also noteworthy that the ACF did not contain any of the mismatch repair or nucleotide excision repair proteins. Interestingly though, Ku antigen and other unexpected proteins including histone deacetylase 6, RPA, histones, among many others, were observed routinely in the mass spectrometry analysis of the ACF (Table 1 and Supplementary Tables S1–S3). Although the non-BER roles of most of these proteins in DNA repair processes is unclear, Ku antigen, XRCC1, DNA Lig III, PARP-1 and PNK have been implicated in forms of DSB repair (78,79), and RPA has been found to bind to BER substrates (80) and to influence the *in vitro* gap filling polymerase activities of X-family polymerases (81,82). Any significance of the pol β ACF proteins in relation to DSB repair pathways remains to be investigated.

SUPPLEMENTARY DATA

Supplementary Data are available at NAR Online: Supplementary Tables 1–3, Supplementary Figures 1–8 and Supplementary Methods.

ACKNOWLEDGEMENTS

The authors thank Julie K. Horton, Michelle Heacock and Bret Freudenthal for reading and commenting on this manuscript, and also Yuan Liu and Vladimir Poltoratsky for their generous help during the course of this study. We thank Bonnie Earnhardt for editorial support.

FUNDING

Intramural Research Program of the National Institutes of Health, National Institute of Environmental Health Sciences, project numbers [Z01ES050158 and Z01ES50159]. Funding for open access charge: Laboratory of Structural Biology, NIEHS.

Conflict of interest statement. None declared.

REFERENCES

1. Klungland,A., Rosewell,I., Hollenbach,S., Larsen,E., Daly,G., Epe,B., Seeberg,E., Lindahl,T. and Barnes,D.E. (1999) Accumulation of premutagenic DNA lesions in mice defective in removal of oxidative base damage. *Proc. Natl Acad. Sci. USA*, **96**, 13300–13305.
2. Lindahl,T. (1982) DNA repair enzymes. *Annu. Rev. Biochem.*, **51**, 61–87.
3. Lindahl,T. and Wood,R.D. (1999) Quality control by DNA repair. *Science*, **286**, 1897–1905.
4. Biade,S., Sobol,R.W., Wilson,S.H. and Matsumoto,Y. (1998) Impairment of proliferating cell nuclear antigen-dependent apurinic/apyrimidinic site repair on linear DNA. *J. Biol. Chem.*, **273**, 898–902.
5. Fortini,P., Pascucci,B., Parlanti,E., Sobol,R.W., Wilson,S.H. and Dogliotti,E. (1998) Different DNA polymerases are involved in the short- and long-patch base excision repair in mammalian cells. *Biochemistry*, **37**, 3575–3580.
6. Frosina,G., Fortini,P., Rossi,O., Carrozzino,F., Raspaglio,G., Cox,L.S., Lane,D.P., Abbondandolo,A. and Dogliotti,E. (1996) Two pathways for base excision repair in mammalian cells. *J. Biol. Chem.*, **271**, 9573–9578.
7. Klungland,A. and Lindahl,T. (1997) Second pathway for completion of human DNA base excision-repair: reconstitution with purified proteins and requirement for DNase IV (FEN1). *EMBO J.*, **16**, 3341–3348.
8. Prasad,R., Dianov,G.L., Bohr,V.A. and Wilson,S.H. (2000) FEN1 stimulation of DNA polymerase beta mediates an excision step in mammalian long patch base excision repair. *J. Biol. Chem.*, **275**, 4460–4466.
9. Demple,B. and Harrison,L. (1994) Repair of oxidative damage to DNA: enzymology and biology. *Annu. Rev. Biochem.*, **63**, 915–948.

10. Mosbaugh,D.W. and Bennett,S.E. (1994) Uracil-excision DNA repair. *Prog. Nucleic Acid Res. Mol. Biol.*, **48**, 315–370.
11. Slupphaug,G., Eftedal,I., Kavli,B., Bharati,S., Helle,N.M., Haug,T., Levine,D.W. and Krokan,H.E. (1995) Properties of a recombinant human uracil-DNA glycosylase from the UNG gene and evidence that UNG encodes the major uracil-DNA glycosylase. *Biochemistry*, **34**, 128–138.
12. Hegde,M.L., Hazra,T.K. and Mitra,S. (2008) Early steps in the DNA base excision/single-strand interruption repair pathway in mammalian cells. *Cell Res.*, **18**, 27–47.
13. Dianov,G., Price,A. and Lindahl,T. (1992) Generation of single-nucleotide repair patches following excision of uracil residues from DNA. *Mol. Cell Biol.*, **12**, 1605–1612.
14. Matsumoto,Y. and Kim,K. (1995) Excision of deoxyribose phosphate residues by DNA polymerase beta during DNA repair. *Science*, **269**, 699–702.
15. Piersen,C.E., Prasad,R., Wilson,S.H. and Lloyd,R.S. (1996) Evidence for an imino intermediate in the DNA polymerase beta deoxyribose phosphate excision reaction. *J. Biol. Chem.*, **271**, 17811–17815.
16. Singhal,R.K., Prasad,R. and Wilson,S.H. (1995) DNA polymerase beta conducts the gap-filling step in uracil-initiated base excision repair in a bovine testis nuclear extract. *J. Biol. Chem.*, **270**, 949–957.
17. Sobol,R.W., Horton,J.K., Kuhn,R., Gu,H., Singhal,R.K., Prasad,R., Rajewsky,K. and Wilson,S.H. (1996) Requirement of mammalian DNA polymerase-beta in base-excision repair. *Nature*, **379**, 183–186.
18. Wiederhold,L., Leppard,J.B., Kedar,P., Karimi-Busheri,F., Rasouli-Nia,A., Weinfeld,M., Tomkinson,A.E., Izumi,T., Prasad,R., Wilson,S.H. *et al.* (2004) AP endonuclease-independent DNA base excision repair in human cells. *Mol. Cell*, **15**, 209–220.
19. Fromme,J.C. and Verdine,G.L. (2004) Base excision repair. *Adv. Protein Chem.*, **69**, 1–41.
20. Khodyreva,S.N., Prasad,R., Ilina,E.S., Sukhanova,M.V., Kutuzov,M.M., Liu,Y., Hou,E.W., Wilson,S.H. and Lavrik,O.I. (2010) Apurinic/apyrimidinic (AP) site recognition by the 5'-dRP/AP lyase in poly(ADP-ribose) polymerase-1 (PARP-1). *Proc. Natl Acad. Sci. USA*, **107**, 22090–22095.
21. Weinfeld,M., Mani,R.S., Abdou,I., Aceytuno,R.D. and Glover,J.N. (2011) Tidying up loose ends: the role of polynucleotide kinase/phosphatase in DNA strand break repair. *Trends Biochem. Sci.*, **36**, 262–271.
22. Caldecott,K.W., McKeown,C.K., Tucker,J.D., Ljungquist,S. and Thompson,L.H. (1994) An interaction between the mammalian DNA repair protein XRCC1 and DNA ligase III. *Mol. Cell Biol.*, **14**, 68–76.
23. Prasad,R., Singhal,R.K., Srivastava,D.K., Molina,J.T., Tomkinson,A.E. and Wilson,S.H. (1996) Specific interaction of DNA polymerase beta and DNA ligase I in a multiprotein base excision repair complex from bovine testis. *J. Biol. Chem.*, **271**, 16000–16007.
24. Prigent,C., Satoh,M.S., Daly,G., Barnes,D.E. and Lindahl,T. (1994) Aberrant DNA repair and DNA replication due to an inherited enzymatic defect in human DNA ligase I. *Mol. Cell Biol.*, **14**, 310–317.
25. Asagoshi,K., Lehmann,W., Braithwaite,E.K., Santana-Santos,L., Prasad,R., Freedman,J.H., Van Houten,B. and Wilson,S.H. (2012) Single-nucleotide base excision repair DNA polymerase activity in C. elegans in the absence of DNA polymerase β. *Nucleic Acids Res.*, **40**, 670–681.
26. Prasad,R., Shock,D.D., Beard,W.A. and Wilson,S.H. (2010) Substrate channeling in mammalian base excision repair pathways: passing the baton. *J. Biol. Chem.*, **285**, 40479–40488.
27. Caldecott,K.W., Tucker,J.D., Stanker,L.H. and Thompson,L.H. (1995) Characterization of the XRCC1-DNA ligase III complex in vitro and its absence from mutant hamster cells. *Nucleic Acids Res.*, **23**, 4836–4843.
28. Luo,H., Chan,D.W., Yang,T., Rodriguez,M., Chen,B.P., Leng,M., Mu,J.J., Chen,D., Songyang,Z., Wang,Y. *et al.* (2004) A new XRCC1-containing complex and its role in cellular survival of methyl methanesulfonate treatment. *Mol. Cell Biol.*, **24**, 8356–8365.
29. Prasad,R., Liu,Y., Deterding,L.J., Poltoratsky,V.P., Kedar,P.S., Horton,J.K., Kanno,S., Asagoshi,K., Hou,E.W., Khodyreva,S.N. *et al.* (2007) HMGB1 is a cofactor in mammalian base excision repair. *Mol. Cell*, **27**, 829–841.
30. Lavrik,O.I., Prasad,R., Sobol,R.W., Horton,J.K., Ackerman,E.J. and Wilson,S.H. (2001) Photoaffinity labeling of mouse fibroblast enzymes by a base excision repair intermediate. Evidence for the role of poly(ADP-ribose) polymerase-1 in DNA repair. *J. Biol. Chem.*, **276**, 25541–25548.
31. Bennett,R.A., Wilson,D.M. 3rd, Wong,D. and Demple,B. (1997) Interaction of human apurinic endonuclease and DNA polymerase beta in the base excision repair pathway. *Proc. Natl Acad. Sci. USA*, **94**, 7166–7169.
32. Kedar,P.S., Kim,S.J., Robertson,A., Hou,E., Prasad,R., Horton,J.K. and Wilson,S.H. (2002) Direct interaction between mammalian DNA polymerase beta and proliferating cell nuclear antigen. *J. Biol. Chem.*, **277**, 31115–31123.
33. Dantzer,F., Schreiber,V., Niedergang,C., Trucco,C., Flatter,E., De La Rubia,G., Oliver,J., Rolli,V., Menissier-de Murcia,J. and de Murcia,G. (1999) Involvement of poly(ADP-ribose) polymerase in base excision repair. *Biochimie*, **81**, 69–75.
34. Plo,I., Liao,Z.Y., Barcelo,J.M., Kohlhagen,G., Caldecott,K.W., Weinfeld,M. and Pommier,Y. (2003) Association of XRCC1 and tyrosyl DNA phosphodiesterase (Tdp1) for the repair of topoisomerase I-mediated DNA lesions. *DNA Repair (Amst.)*, **2**, 1087–1100.
35. Das,A., Wiederhold,L., Leppard,J.B., Kedar,P., Prasad,R., Wang,H., Boldogh,I., Karimi-Busheri,F., Weinfeld,M., Tomkinson,A.E. *et al.* (2006) NEIL2-initiated, APE-independent repair of oxidized bases in DNA: evidence for a repair complex in human cells. *DNA Repair (Amst.)*, **5**, 1439–1448.
36. Mendez,F., Sandigursky,M., Franklin,W.A., Kenny,M.K., Kureekattil,R. and Bases,R. (2000) Heat-shock proteins associated with base excision repair enzymes in HeLa cells. *Radiat. Res.*, **153**, 186–195.
37. Seo,Y.R., Fishel,M.L., Amundson,S., Kelley,M.R. and Smith,M.L. (2002) Implication of p53 in base excision DNA repair: in vivo evidence. *Oncogene*, **21**, 731–737.
38. Zhou,J., Ahn,J., Wilson,S.H. and Prives,C. (2001) A role for p53 in base excision repair. *EMBO J.*, **20**, 914–923.
39. Balakrishnan,L., Brandt,P.D., Lindsey-Boltz,L.A., Sancar,A. and Bambara,R.A. (2009) Long patch base excision repair proceeds via coordinated stimulation of the multienzyme DNA repair complex. *J. Biol. Chem.*, **284**, 15158–15172.
40. Gembka,A., Toueille,M., Smirnova,E., Poltz,R., Ferrari,E., Villani,G. and Hubscher,U. (2007) The checkpoint clamp, Rad9-Rad1-Hus1 complex, preferentially stimulates the activity of apurinic/apyrimidinic endonuclease 1 and DNA polymerase beta in long patch base excision repair. *Nucleic Acids Res.*, **35**, 2596–2608.
41. Toueille,M., El-Andaloussi,N., Frouin,I., Freire,R., Funk,D., Shevelev,I., Friedrich-Heineken,E., Villani,G., Hottiger,M.O. and Hubscher,U. (2004) The human Rad9/Rad1/Hus1 damage sensor clamp interacts with DNA polymerase beta and increases its DNA substrate utilisation efficiency: implications for DNA repair. *Nucleic Acids Res.*, **32**, 3316–3324.
42. Narayan,S., Jaiswal,A.S. and Balusu,R. (2005) Tumor suppressor APC blocks DNA polymerase beta-dependent strand displacement synthesis during long patch but not short patch base excision repair and increases sensitivity to methylmethane sulfonate. *J. Biol. Chem.*, **280**, 6942–6949.
43. Sobol,R.W., Prasad,R., Evenski,A., Baker,A., Yang,X.P., Horton,J.K. and Wilson,S.H. (2000) The lyase activity of the DNA repair protein beta-polymerase protects from DNA-damage-induced cytotoxicity. *Nature*, **405**, 807–810.
44. Horton,J.K., Stefanick,D.F. and Wilson,S.H. (2005) Involvement of poly(ADP-ribose) polymerase activity in regulating Chk1-dependent apoptotic cell death. *DNA Repair (Amst.)*, **4**, 1111–1120.
45. Horton,J.K., Prasad,R., Hou,E. and Wilson,S.H. (2000) Protection against methylation-induced cytotoxicity by DNA polymerase beta-dependent long patch base excision repair. *J. Biol. Chem.*, **275**, 2211–2218.

46. Pourquier,P. and Pommier,Y. (2001) Topoisomerase I-mediated DNA damage. *Adv. Cancer Res.*, **80**, 189–216.
47. Loeb,L.A. and Preston,B.D. (1986) Mutagenesis by apurinic/apyrimidinic sites. *Annu. Rev. Genet.*, **20**, 201–230.
48. Simonelli,V., Narciso,L., Dogliotti,E. and Fortini,P. (2005) Base excision repair intermediates are mutagenic in mammalian cells. *Nucleic Acids Res.*, **33**, 4404–4411.
49. Cannavo,E., Gerrits,B., Marra,G., Schlapbach,R. and Jiricny,J. (2007) Characterization of the interactome of the human MutL homologues MLH1, PMS1, and PMS2. *J. Biol. Chem.*, **282**, 2976–2986.
50. Puig,O., Caspary,F., Rigaut,G., Rutz,B., Bouveret,E., Bragado-Nilsson,E., Wilm,M. and Seraphin,B. (2001) The tandem affinity purification (TAP) method: a general procedure of protein complex purification. *Methods*, **24**, 218–229.
51. Beard,W.A. and Wilson,S.H. (1995) Purification and domain-mapping of mammalian DNA polymerase beta. *Methods Enzymol.*, **262**, 98–107.
52. Strauss,P.R., Beard,W.A., Patterson,T.A. and Wilson,S.H. (1997) Substrate binding by human apurinic/apyrimidinic endonuclease indicates a Briggs-Haldane mechanism. *J. Biol. Chem.*, **272**, 1302–1307.
53. Wang,Y.C., Burkhart,W.A., Mackey,Z.B., Moyer,M.B., Ramos,W., Husain,I., Chen,J., Besterman,J.M. and Tomkinson,A.E. (1994) Mammalian DNA ligase II is highly homologous with vaccinia DNA ligase. Identification of the DNA ligase II active site for enzyme-adenylate formation. *J. Biol. Chem.*, **269**, 31923–31928.
54. Prasad,R., Beard,W.A., Strauss,P.R. and Wilson,S.H. (1998) Human DNA polymerase beta deoxyribose phosphate lyase. Substrate specificity and catalytic mechanism. *J. Biol. Chem.*, **273**, 15263–15270.
55. Watters,D., Khanna,K.K., Beamish,H., Birrell,G., Spring,K., Kedar,P., Gatei,M., Stenzel,D., Hobson,K., Kozlov,S. *et al.* (1997) Cellular localisation of the ataxia-telangiectasia (ATM) gene product and discrimination between mutated and normal forms. *Oncogene*, **14**, 1911–1921.
56. Theriot,C.A., Hegde,M.L., Hazra,T.K. and Mitra,S. (2010) RPA physically interacts with the human DNA glycosylase NEIL1 to regulate excision of oxidative DNA base damage in primer-template structures. *DNA Repair*, **9**, 643–652.
57. Kutuzov,M.M., Ilina,E.S., Sukhanova,M.V., Pyshnaya,I.A., Pyshnyi,D.V., Lavrik,O.I. and Khodyreva,S.N. (2011) Interaction of poly(ADP-ribose) polymerase 1 with apurinic/apyrimidinic sites within clustered DNA damage. *Biochemistry (Mosc.)*, **76**, 147–156.
58. Habraken,Y. and Verly,W.G. (1986) Chromatin 3'-phosphatase/5'-OH kinase cannot transfer phosphate from 3' to 5' across a strand nick in DNA. *Nucleic Acids Res.*, **14**, 8103–8110.
59. Jilani,A., Ramotar,D., Slack,C., Ong,C., Yang,X.M., Scherer,S.W. and Lasko,D.D. (1999) Molecular cloning of the human gene, PNKP, encoding a polynucleotide kinase 3'-phosphatase and evidence for its role in repair of DNA strand breaks caused by oxidative damage. *J. Biol. Chem.*, **274**, 24176–24186.
60. Whitehouse,C.J., Taylor,R.M., Thistlethwaite,A., Zhang,H., Karimi-Busheri,F., Lasko,D.D., Weinfeld,M. and Caldecott,K.W. (2001) XRCC1 stimulates human polynucleotide kinase activity at damaged DNA termini and accelerates DNA single-strand break repair. *Cell*, **104**, 107–117.
61. Lee,Y., Katyal,S., Li,Y., El-Khamisy,S.F., Russell,H.R., Caldecott,K.W. and McKinnon,P.J. (2009) The genesis of cerebellar interneurons and the prevention of neural DNA damage require XRCC1. *Nat. Neurosci.*, **12**, 973–980.
62. Liu,L.F. (1989) DNA topoisomerase poisons as antitumor drugs. *Annu. Rev. Biochem.*, **58**, 351–375.
63. Shen,J., Gilmore,E.C., Marshall,C.A., Haddadin,M., Reynolds,J.J., Eyaid,W., Bodell,A., Barry,B., Gleason,D., Allen,K. *et al.* (2010) Mutations in PNKP cause microcephaly, seizures and defects in DNA repair. *Nat. Genet.*, **42**, 245–249.
64. Debethune,L., Kohlhagen,G., Grandas,A. and Pommier,Y. (2002) Processing of nucleopeptides mimicking the topoisomerase I-DNA covalent complex by tyrosyl-DNA phosphodiesterase. *Nucleic Acids Res.*, **30**, 1198–1204.
65. Pouliot,J.J., Yao,K.C., Robertson,C.A. and Nash,H.A. (1999) Yeast gene for a Tyr-DNA phosphodiesterase that repairs topoisomerase I complexes. *Science*, **286**, 552–555.
66. Wang,J.C. (1996) DNA topoisomerases. *Annu. Rev. Biochem.*, **65**, 635–692.
67. El-Khamisy,S.F. and Caldecott,K.W. (2006) TDP1-dependent DNA single-strand break repair and neurodegeneration. *Mutagenesis*, **21**, 219–224.
68. Akbari,M., Solvang-Garten,K., Hanssen-Bauer,A., Lieske,N.V., Pettersen,H.S., Pettersen,G.K., Wilson,D.M. 3rd, Krokan,H.E. and Otterlei,M. (2010) Direct interaction between XRCC1 and UNG2 facilitates rapid repair of uracil in DNA by XRCC1 complexes. *DNA Repair (Amst.)*, **9**, 785–795.
69. Caldecott,K.W. (2003) Protein-protein interactions during mammalian DNA single-strand break repair. *Biochem. Soc. Trans.*, **31**, 247–251.
70. Hanssen-Bauer,A., Solvang-Garten,K., Sundheim,O., Pena-Diaz,J., Andersen,S., Slupphaug,G., Krokan,H.E., Wilson,D.M. 3rd, Akbari,M. and Otterlei,M. (2011) XRCC1 coordinates disparate responses and multiprotein repair complexes depending on the nature and context of the DNA damage. *Environ. Mol. Mutagen.*, **52**, 623–635.
71. Takanami,T., Nakamura,J., Kubota,Y. and Horiuchi,S. (2005) The Arg280His polymorphism in X-ray repair cross-complementing gene 1 impairs DNA repair ability. *Mut. Res.*, **582**, 135–145.
72. Takashima,H., Boerkoel,C.F., John,J., Saifi,G.M., Salih,M.A., Armstrong,D., Mao,Y., Quiocho,F.A., Roa,B.B., Nakagawa,M. *et al.* (2002) Mutation of TDP1, encoding a topoisomerase I-dependent DNA damage repair enzyme, in spinocerebellar ataxia with axonal neuropathy. *Nat. Genet.*, **32**, 267–272.
73. Almeida,K.H. and Sobol,R.W. (2007) A unified view of base excision repair: lesion-dependent protein complexes regulated by post-translational modification. *DNA Repair (Amst.)*, **6**, 695–711.
74. Caldecott,K.W. (2008) Single-strand break repair and genetic disease. *Nat. Rev. Genet.*, **9**, 619–631.
75. Dianova,II., Sleeth,K.M., Allinson,S.L., Parsons,J.L., Breslin,C., Caldecott,K.W. and Dianov,G.L. (2004) XRCC1-DNA polymerase beta interaction is required for efficient base excision repair. *Nucleic Acids Res.*, **32**, 2550–2555.
76. El-Khamisy,S.F., Masutani,M., Suzuki,H. and Caldecott,K.W. (2003) A requirement for PARP-1 for the assembly or stability of XRCC1 nuclear foci at sites of oxidative DNA damage. *Nucleic Acids Res.*, **31**, 5526–5533.
77. Liu,Y., Prasad,R., Beard,W.A., Kedar,P.S., Hou,E.W., Shock,D.D. and Wilson,S.H. (2007) Coordination of steps in single-nucleotide base excision repair mediated by apurinic/apyrimidinic endonuclease 1 and DNA polymerase beta. *J. Biol. Chem.*, **282**, 13532–13541.
78. Della-Maria,J., Zhou,Y., Tsai,M.S., Kuhnlein,J., Carney,J.P., Paull,T.T. and Tomkinson,A.E. (2011) Human Mre11/human Rad50/Nbs1 and DNA ligase IIIalpha/XRCC1 protein complexes act together in an alternative nonhomologous end joining pathway. *J. Biol. Chem.*, **286**, 33845–33853.
79. Mansour,W.Y., Rhein,T. and Dahm-Daphi,J. (2010) The alternative end-joining pathway for repair of DNA double-strand breaks requires PARP1 but is not dependent upon microhomologies. *Nucleic Acids Res.*, **38**, 6065–6077.
80. Lavrik,O.I., Nasheuer,H.P., Weisshart,K., Wold,M.S., Prasad,R., Beard,W.A., Wilson,S.H. and Favre,A. (1998) Subunits of human replication protein A are crosslinked by photoreactive primers synthesized by DNA polymerases. *Nucleic Acids Res.*, **26**, 602–607.
81. Belousova,E.A., Maga,G., Fan,Y., Kubareva,E.A., Romanova,E.A., Lebedeva,N.A., Oretskaya,T.S. and Lavrik,O.I. (2010) DNA polymerases beta and lambda bypass thymine glycol in gapped DNA structures. *Biochemistry*, **49**, 4695–4704.
82. Locatelli,G.A., Pospiech,H., Tanguy Le Gac,N., van Loon,B., Hubscher,U., Parkkinen,S., Syvaoja,J.E. and Villani,G. (2010) Effect of 8-oxoguanine and abasic site DNA lesions on in vitro elongation by human DNA polymerase in the presence of replication protein A and proliferating-cell nuclear antigen. *Biochem. J.*, **429**, 573–582.